JOURNAL OF GEOPHYSICAL RESEARCH, VOL. 104, NO. D22, PAGES 27,735–27,754, NOVEMBER 27, 1999

Net primary productivity distribution in the BOREAS region from a process model using satellite and surface data

J. Liu, J. M. Chen, J. Cihlar, and W. Chen

Canada Centre for Remote Sensing, Ottawa

Abstract. The purpose of this paper is to upscale tower measurements of net primary productivity (NPP) to the Boreal Ecosystem-Atmosphere Study (BOREAS) study region by means of remote sensing and modeling. The Boreal Ecosystem Productivity Simulator (BEPS) with a new daily canopy photosynthesis model was first tested in one coniferous and one deciduous site. The simultaneous CO_2 flux measurements above and below the tree canopy made it possible to isolate daily net primary productivity of the tree canopy for model validation. Soil water holding capacity and gridded daily meteorological data for the region were used as inputs to BEPS, in addition to 1 km resolution land cover and leaf area index (LAI) maps derived from the advanced very high resolution radiometer (AVHRR) data. NPP statistics for the various cover types in the BOREAS region and in the southern study area (SSA) and the northern study area (NSA) are presented. Strong dependence of NPP on LAI was found for the three major cover types: coniferous forest, deciduous forest and cropland. Since BEPS can compute total photosynthetically active radiation absorbed by the canopy in each pixel, light use efficiencies for NPP and gross primary productivity could also be analyzed. From the model results, the following area-averaged statistics were obtained for 1994: (1) mean NPP for the BOREAS region of 217 g C m^{-2} yr^{-1}; (2) mean NPP of forests (excluding burnt areas in the region) equal to 234 g C m^{-2} yr^{-1}; (3) mean NPP for the SSA and the NSA of 297 and 238 g C m^{-2} yr^{-1}, respectively; and (4) mean light use efficiency for NPP equal to 0.40, 0.20, and 0.33 g C (MJ APAR)$^{-1}$ for deciduous forest, coniferous forest, and crops, respectively.

1. Introduction

The Boreal Ecosystem-Atmosphere Study(BOREAS) was a large-scale international and interdisciplinary research program, involving over 80 science teams from five countries [*Sellers et al.*, 1995, 1997]. The goal of BOREAS was to improve our understanding of the interactive processes between the boreal forest and the atmosphere in order to assess their roles in global change. Between 1994 and 1996, detailed measurements were made at multiple spatial scales, ranging from leaves and twigs (~10^{-5} m^2 – 10^{-1} m^2), plots (~1 m^2 – 100 m^2), tower flux sites (~1 km^2), and study areas (~10^3 km^2) to the study region (~10^6 km^2). These data provide unprecedented opportunities to explore many ecological processes and to address issues concerning the role of boreal ecosystems in global carbon cycle. Integration of the data in the spatial and temporal domains can maximize the potential of the data set and is necessary for achieving the goal of BOREAS.

A key component of the terrestrial carbon cycle is net primary productivity (NPP), defined as the net amount of new carbon absorbed by plants per unit space and time. Although detailed NPP studies have been conducted at individual BOREAS sites [*Black et al., 1996; Frolking, 1997; Kimball et al, 1997; Gower et al., 1997; Steele et al., 1997; Ryan et al.*, 1997], the spatial distribution of NPP over the entire study region has not yet been mapped through mechanistic integration of the BOREAS data and upscaling to the study region.

Currently, two types of models are used for mapping NPP at regional or global scales. Some simulate plant physiological processes on the basis of biophysical and biochemical principles [*Running et al.*, 1989; *Bonan*, 1995; *Melillo et al.*, 1995; *Woodward et al.*, 1995; *Foley*, 1994; *Denning et al.*, 1996; *Liu et al.*, 1997]. Another approach is to determine NPP using photosynthetically active radiation absorbed by plants (APAR) and a light use efficiency (LUE) [*Potter et al.*, 1993; *Ruimy et al.*, 1994]. The LUE models of *Prince and Goward* [1995] and *Goetz et al.* [this issue] use APAR to derive potential photosynthesis (Pg), stress terms to reduce Pg to actual rates, and biomass and temperature to estimate autotrophic respiration. LUE models have the advantage of high computation efficiency and low demand on input data. On the other hand, they considerably simplify ecophysiological and biochemical processes in plant canopies. In contrast, process models explicitly simulate these processes, providing an alternative in remote sensing applications. Models that are more process-oriented have the advantages of allowing investigations of the interaction between the biosphere and the atmosphere and to predict the impacts of climate change on ecosystems and their feedbacks to the climate system.

The primary objectives of this study are (1) to show the NPP distribution in the BOREAS region calculated by using a process model, (2) to investigate the needs and limitations of methods for scaling from tower sites to the region, (3) to discuss the spatial distribution of NPP in relationship to

Paper number 1999JD900768.
0148-0227/99/1999JD900768$09.00

biological characteristics of plants and environmental conditions in the region, and (4) to provide independent estimates of the LUE and the variability in LUE of the major boreal cover types in the region.

The NPP distribution was determined with a process-based model, namely, the Boreal Ecosystem Productivity Simulator (BEPS) [*Liu et al.*, 1997]. BEPS was refined by replacing the analog-based photosynthesis model [*Running and Coughlan*, 1988] with the Farquhar model [*Farquhar et al.*, 1980]. In addition, to enable use of a leaf-level photosynthesis model with remote sensing measurements, a new spatial and temporal scaling scheme was also developed [*Chen et al.*, 1999a].

2. BEPS Description

2.1 Overview

BEPS was developed on the basis of the Forest BioGeochemical Cycles (Forest-BGC) model [*Running and Coughlan*, 1988]. Two major modifications were made to Forest-BGC to adapt it to the boreal environment [*Liu et al.*, 1997]: (1) inclusion of an advanced canopy radiation model to describe the specific boreal canopy architecture; and (2) adjustments of biophysical and biochemical parameters for the main boreal land cover types. Computationally, BEPS differs from the original version of the Forest-BGC [*Running and Coughlan*, 1988] in several respects: (1) it extends stand-level calculations to a large area (watershed, province, or a region) using gridded meteorological and soil data rather than single weather station data; (2) land cover information derived from satellite data is used to set biophysical and biochemical parameters; and (3) satellite data are used to provide the spatial and seasonal distributions of LAI. In addition to the satellite data, the model requires input of daily meteorological data (radiation, temperature, humidity, and precipitation) and soil data (available water-holding capacity). The temporal interval is daily for meteorological data, 10 days for LAI, and annual for land cover. BEPS integrates the input data and produces output of NPP and other carbon and water cycle components such as autotrophic respiration and evapotranspiration. The computation was made pixel by pixel in daily time steps assuming vegetation and environment conditions were uniform within each pixel, currently being 1 km^2.

2.2 An Improvement on Photosynthesis Rate Modeling

NPP is estimated from gross primary productivity (GPP) and autotropic respiration (R_a):

$$\mathrm{NPP} = \mathrm{GPP} - R_a. \tag{1}$$

In this study, BEPS was modified to incorporate Farquhar's model [*Farquhar et al.*, 1980] for GPP calculation. This modification is similar to the transformation from Forest-BGC to Biome-BGC [*Hunt and Running*, 1992; *Running and Hunt*, 1993] and from the Simple Biosphere model 1 (SiB1) to SiB2 [*Sellers et al.*, 1996]. Farquhar's model provides a framework for evaluating the effects of the changes in CO_2 concentration, temperature, and other factors on photosynthesis. However, to use this leaf-level photosynthesis model for regional remote sensing applications, two major challenges must be overcome: (1) large temporal variability in meteorological conditions (radiation, temperature, and humidity) exists within a given time step (daily or longer), and a nonlinear response of leaf photosynthesis to meteorological conditions can introduce large errors in the NPP calculations; and (2) leaves in different positions in the canopy are not uniformly exposed to the Sun at any given time, thus requiring vertical integration in the canopy.

The first challenge can be avoided if a model is run at small time steps (seconds to minutes). To date, most global carbon budget models using Farquhar's approach were implemented at time steps of minutes to hours to avoid the need for temporal integration, and at coarse spatial resolution (0.5°-2°) to reduce computing demand [*Bonan*, 1995; *Denning et al., 1996; Foley et al.*, 1996]. The inherent limitation of this low-resolution approach is the large spatial heterogeneity. The use of remote sensing data at moderate to high spatial resolutions (~1 km) can greatly reduce this problem, but it dramatically increases the computational demand. Data availability is often a problem for small time step computations for large areas, especially when a model is run independently of a numerical weather simulation model. Therefore a practical solution for using satellite data at moderate to high spatial resolutions with the available daily meteorological data is to compute photosynthesis at daily steps with proper consideration of diurnal variability of weather conditions.

From the BOREAS field data (see below) it was found that because of the nonlinear response of leaf photosynthesis to meteorological variables, simply by using arithmetic daily means of the variables will result in large errors in daily photosynthesis calculations. To avoid the errors, a daily NPP model was developed with a new temporal and spatial integration scheme [*Chen et al.*, 1999a]. A brief description is given below.

The Farquhar's model describes the instantaneous leaf gross photosynthesis rate for C_3 plants as the minimum of

$$W_c = V_m \frac{C_i - \Gamma}{C_i + K}, \tag{2a}$$

$$W_j = J \frac{C_i - \Gamma}{4.5C_i + 10.5\Gamma}, \tag{2b}$$

where W_c and W_j are Rubisco-limited and light-limited gross photosynthesis rate in μmol m^{-2} s^{-1}, respectively. V_m is the maximum carboxylation rate in μmol m^{-2} s^{-1}; J is the radiation-dependent electron transport rate in μmol m^{-2} s^{-1}; C_i is intercellular CO_2 concentration; Γ is temperature-dependent CO_2 compensation point without dark respiration; and K is a temperature-dependent function of enzyme kinetics. The unit for C_i, Γ, K can be either in Pascal (Pa) or in ppmv (parts per million by volume). The procedure to calculate all the parameters is described in Table 1. Symbols and their definitions and units are listed in the Notation section.

To obtain the net CO_2 assimilation rate (A), daytime leaf dark respiration (R_d) is subtracted from equation (2):

$$A = \min(W_c, W_j) - R_d. \tag{3}$$

According to fluid physics, the photosynthesis rate can also be described in the form

$$A = (C_a - C_i)g \,, \tag{4}$$

where C_a is CO_2 concentration in the atmosphere, and g is the conductance to CO_2 from the leaf cells to the atmosphere outside of leaf boundary layer in μmol m^{-2} s^{1} Pa^{-1}.

$$g \approx 10^6 g_s /(R_{gas}(T_a + 273)) \,, \tag{5}$$

where g_s is stomatal conductance in m s^{-1}; R_{gas} is the molar gas constant, equal to 8.3143 m^3 Pa mol^{-1} K^{-1}; and T is the air temperature in °C. Combining equations (2), (3), and (4) and choosing the solution of the quadratic equations with the smaller roots, we obtain the net CO_2 assimilation rate as

$$A = \frac{1}{2}(a^{1/2}g + c^{1/2} - \sqrt{ag^2 + bg + c}) \,, \tag{6}$$

where A is the minimum of A_c and A_j, corresponding to W_c and W_j. For A_c, $a = (K+C_a)^2$, $b = 2(2\Gamma+K-C_a)V_m+2(C_a+K)R_d$, and $c=(V_m-R_d)^2$ and for A_j, $a = (2.3\Gamma+C_a)^2$, $b = 0.4(4.3\Gamma-C_a)J+2(C_a+2.3\Gamma)R_d$, and $c=(0.2J-R_d)^2$.

Theoretically, the diurnal integration of A_c and A_j for daily total photosynthesis should be made with respect to time. Our attempt to obtain an analytical solution to such an integration was not successful because of the complication introduced by the nonlinear relationship between time and stomatal conductance, which is approximately sinusoidal. We therefore found an alternative by integrating with respect to conductance (g). The major assumptions are that the daily course of solar radiation follows a cosine function of solar zenith angle with a peak at solar noon and that this variation determines the diurnal pattern of stomatal conductance. Therefore daily averaged A can be obtained from

$$A = \frac{\mu}{2g_n}\int_0^{g_n}[a^{1/2}g + c^{1/2} - \sqrt{ag^2 + bg + c}]dg \,, \tag{7}$$

where g_n is the conductance at noon, and μ is a coefficient for adjusting nonlinear change of g with time. It can be calculated from

$$\mu = \frac{1}{0.5\pi/2}\int_0^{\pi/2}\cos\theta d\theta = \frac{4}{\pi} \approx 1.27 \,. \tag{8}$$

Finally, equation (7) is solved analytically:

$$A = \frac{1.27}{2g_n}\left(\frac{a^{1/2}}{2}g_n^2 + c^{1/2}g_n - \frac{2ag_n + b}{4a}d + \frac{b}{4a}c^{1/2} + \frac{b^2 - 4ac}{8a^{3/2}}\ln\frac{2ag_n + b + 2a^{1/2}d}{b + 2a^{1/2}c^{1/2}}\right) \,, \tag{9}$$

where $d=(ag_n^2 + bg_n+c)^{1/2}$. It is noted that (1) no additional parameters are introduced in this daily model, all the constants are determined by the leaf biochemical parameters in the original Farquhar model (see Table 1); (2) although equation (9) appears to be complex, it is numerically stable, and no numerical problems have been encountered in its use over large areas and under extreme conditions; (3) the analytical integration given by equation (9) is computationally efficient and avoids a daily loop using a numerical integration method.

For the spatial integration from leaf to canopy, a method for stratifying a canopy into sunlit and shaded leaf components has been used to upscale Farquhar's model. This is a preferable approach because the largest difference in leaf illumination in a canopy exists between sunlit and shaded leaves. The daily integration of A_c and A_j can then be made separately for each component. The calculation of sunlit leaf area and shaded leaf area is based on *Norman* [1982], with some modifications. One of the important modifications is the consideration of forest clumping index (see Table 2 in detail).

The stomatal conductance at noon can be estimated by a species-dependent maximum, which is reduced by the departure of environmental conditions from the optimum [*Jarvis*, 1976; *Baldocchi et al.*, 1987; *Running and Coughlan*, 1988]. The reduction is described by a set of environmental functions, including photosynthetic photon flux density (PPFD), temperature (T), vapor pressure deficit (VPD), and leaf water potential (LWP); that is,

$$g_s = g_{s,max} f(\text{PPFD}) f(T) f(\text{VPD}) f(\text{LWP}) \,, \tag{10}$$

where the environmental functions produce scalars between 0 and 1. Leaf water potential can be derived from relative soil moisture [*Running and Coughlan*, 1988], i. e., LWP=0.2/(volumetric soil water content/soil water holding capacity). Equation (10) considers the environmental constraints to stomatal conductance in a way similar to NPP formulations in a LUE model which forces the maximum NPP to the actual rates using stress terms [*Goetz et al.*, this issue; *Prince and Goward*, 1995]. However, equation (10) describes stomatal conductance at leaf level, and the environmental functions can be determined with measurements, while the formulation of NPP in the LUE model is at stand level and it is difficult to resolve the environmental functions experimentally. Figure 1 shows the environmental functions based on *Jarvis* and *Morison* [1981], *Baldocchi et al.* [1987], *Bonan* [1995], and *Dang et al* [1997]. Equations for some of the functions are also given by *Chen et al.* [1999a].

2.3 Autotrophic Respiration

Autotrophic respiration (R_a) is separated into maintenance respiration (R_m) and growth respiration (R_g) [*Ryan*, 1990; *Running and Coughlan*, 1988]:

$$R_a = R_m + R_g = \sum_i (R_{m,i} + R_{g,i}) \,, \tag{11}$$

where i defines a plant component (1 for leaf, 2 for stem, and 3 for root). Maintenance respiration is temperature-dependent:

$$R_{m,i} = M_i r_{m,i} Q_{10}^{(T-Tb)/10} \,, \tag{12}$$

where M_i is biomass (sapwood for stems) of a plant component i; $r_{m,i}$ is maintenance respiration coefficient for component i, or respiration rate at base temperature; Q_{10} is the temperature sensitivity factor, and T_b is the base temperature. Growth respiration is generally considered to be independent of temperature and is proportional to GPP:

$$R_{g,i} = r_{g,i} r_{a,i} \text{GPP} \,, \tag{13}$$

Table 1. Procedure to Calculate Parameters in the Farquhar Model

Step	Equation	Reference
1	K_c (Michaelis_Menton constant for CO_2) and K_o (Michaelis_Menton constant for O_2) $K_c = 30 \times 2.1^{(T-25)/10}$ $K_o = 30{,}000 \times 1.2^{(T-25)/10}$	*Collatz et. al.* [1991]
2	K (function of enzyme kinetics) $K=K_c(1+O_2/K_o)$	*Farquhar et al.* [1980]
3	Γ (CO_2 compensation point in the absence of dark respiration) $\Gamma = 4.04 \times (1.75)^{(T-25)/10}$	*Collatz et al.* [1991] *Sellers et al.* [1992]
4	V_m (the maximum carboxylation rate) $f(T)=1/(1+\exp((-220{,}000+710(T+273))/(R_{gas}(T+273))))$ $f(N)=N/N_m$ $V_m = V_{m25}\, 2.4^{(T-25)/10} f(T) f(N)$	*Bonan* [1995]
5	J (electron transport rate) $J_{max}=29.1+1.64V_m$ $J=J_{max}\mathrm{PPFD}/(\mathrm{PPFD}+2.1J_{max})$	*Wullschleger* [1993] *Farquhar and Caemmerer* [1982]
6	R_d (daytime leaf dark respiration) $R_d=0.015V_m$	*Collatz et al.* [1991]

where $r_{g,i}$ is a growth respiration coefficient for plant component i, and $r_{a,i}$ is carbon allocation fraction for plant component i.

In this study, Q_{10} and T_b are set to 2.3 and 20°C, respectively. Biomass and respiration coefficients are determined on the basis of earlier BOREAS studies [*Gower et al.*, 1997; *Kimball et al.*, 1997; *Lavigne and Ryan*, 1997; *Ryan et al.*, 1997; *Steele et al.*, 1997]. The coefficients and biomass vary among land cover types (see below). The carbon allocation fraction is the same as in Forest-BGC for leaf, stem, and root [*Running and Coughlan*, 1988].

3. Validation of BEPS With BOREAS Data

Modeled NPP results are often validated annually using biomass measurements, but are rarely validated on a daily basis because of the difficulty in measuring daily NPP. However, if daily CO_2 flux data above and below a plant canopy are available, it becomes possible to obtain the "measured" daily NPP of the tree canopy (overstory) from the data. The term "overstory" is used to separate the tree canopy from the understory, including shrubs, grasses, and mosses. The fluxes at the two levels can be expressed as the sums of several components:

$$FLUX_A = P_{OVER} + P_{UNDER} + R_{OVER,ABOVE} + R_{OVER,ROOT} + R_{UNDER} + R_{SOIL}, \quad (14)$$

$$FLUX_B = P_{UNDER} + R_{OVER,ROOT} + R_{UNDER} + R_{SOIL}, \quad (15)$$

where $FLUX_A$ is the flux above the canopy, and $FLUX_B$ is the flux below the canopy. P and R denote photosynthesis and respiration fluxes, respectively. The subscripts *OVER*, *UNDER*, and *SOIL* indicate overstory, understory and soil. The subscripts *ABOVE* and *ROOT* are for above ground and root of the overstory. We define downward fluxes as positive and upward fluxes as negative so photosynthesis is always positive and respiration is always negative. Therefore NPP of the overstory, defined as $P_{OVER} + R_{OVER,ABOVE} + R_{OVER,ROOT}$, can be obtained from

$$NPP = FLUX_A - FLUX_B + R_{OVER,ROOT}. \quad (16)$$

Root respiration is involved in the equation because of the transport of carbon to roots, in turn, released from the soil surface. It can be estimated from equations (12) and (13). Note that the term R_{SOIL} for the heterotrophic respiration in soil appears in equations (14) and (15) and is eliminated after taking the difference between these two equations. This is the major advantage of this NPP validation technique. This approach eliminates the complexity of estimating soil respiration and the contribution of the understory to the carbon cycle.

During BOREAS, CO_2 flux measurements above and below the plant canopy were made at the old black spruce

Table 2. Procedure to Calculate Leaf Area Index and Irradiance for Sunlit and Shade Leaves

Step	Equation	Reference
1	θ (daily mean solar zenith angle)	*Oke* [1990]
	θ_n=arccos(sin(-23.4cos(360(D +10)/365))sinφ + cos(-23.4cos(360(D+10)/365))cosφ)	
	θ=((π/2+θ_n)/2+θ_n)/2	
2	LAI_{sun} (sunlit leaf area index) and LAI_{shade} (shaded leaf area index)	*Norman* [1982] *Chen et al.* [1999a]
	$LAI_{sun} = 2\cos\theta(1-\exp(-0.5\Omega LAI/\cos\theta))$	
	$LAI_{shade} = LAI - LAI_{sun}$	
3	S_{dir} (direct solar irradiance) and S_{dif} (diffuse solar irradiance)	*Erbs et al.* [1982] *Black et al.* [1991]
	$R = S_g/(S_o\cos\theta)$	
	$\frac{S_{dif}}{S_g} = \begin{cases} 0.943 + 0.734R - 4.9R^2 + 1.796R^3 + 2.058R^4 & R < 0.8 \\ 0.13 & R > 0.8 \end{cases}$	
	$S_{dir}=S_g-S_{dif}$	
4	C (irradiance from multiple scattering of direct radiation)	*Norman* [1982] *Chen et al.* [1999a]
	$\cos\bar{\theta} = 0.537+0.025LAI$	
	$S_{dif,under}=S_{dif}\exp(-0.5\Omega LAI/\cos\bar{\theta})$	
	$C = 0.07\Omega S_{dir}(1.1-0.1LAI)\exp(-\cos\theta)$	
5	S_{sun} (sunlit-leaf irradiance) and S_{shade} (shaded leaf irradiance)	*Norman* [1982] *Chen et al.* [1999a]
	$S_{shade}=(S_{dif}-S_{dif,\,under})/LAI + C$	
	$S_{sun} = S_{dir}\cos\alpha/\cos\theta + S_{shade}$	

(NOBS) site in the northern study area (NSA) in 1996 and at the old aspen site (SOA) in the southern study area (SSA) in 1994 [*Black et al.*, 1996; *Goulden et al.*, 1997; *Goulden and Crill*, 1997]. At the spruce site, both tower flux measurements over the canopy and chamber measurements at the surface (including the understory) were made simultaneously. The data were checked for quality [*Goulden and Crill*, 1997] and good data from May 28 to October 21, 1996, were used in this study. The chamber measurements were made at 3-hour intervals with two chambers for feather moss and three chambers for sphagnum moss. The same principles given in equations (14), (15) and (16) were also used to obtain the overstory NPP from simultaneous eddy-covariance measurements in the old aspen stand at two heights: one above the forest and one between the overstory and the understory. More details of the measurement procedures and the data set in 1994 are given by *Black et al.* [1996]. For both sites, originally measured raw flux data were summed to daily totals. No correction was made for nighttime eddy-covariance measurements because even when the upward CO_2 flux was low at night with low friction velocity, CO_2 emission due to root and soil respiration would be stored in the soil and air column within the canopy. This CO_2 storage would be eventually released and detected by the instrument when the wind speed was restored [*Chen et al.*, 1999b]. Therefore the calm-night flux correction was not made for a daily summation. For the NOBS chamber measurements, 50% weight was given to the average of two chambers for feather moss and 50% weight to the average of three chambers for sphagnum moss. This weight distribution reflects the percentage coverage of these two moss types on the forest floor. Details on site conditions, data processing, and parameterization for the species are available in the work of *Chen et al.* [1999a].

For both NOBS and SOA sites, the daily NPP values calculated from the two-level measurements according to equation (16) are referred to as the "measured daily NPP". The largest uncertainty in the daily NPP values exists in root respiration estimation, but auxiliary site measurements have helped reduce the uncertainty. Root respiration at these two sites was estimated from equations (12) and (13) using respiration coefficients of Biome-BGC [*Kimball et al.*, 1997] and root biomass data of *Steele et al.* [1997]. The estimated annual total root respiration agrees within 15% with measurements reported by *Ryan et al.* [1997]. The comparison of our model results with the measured daily NPP at these two

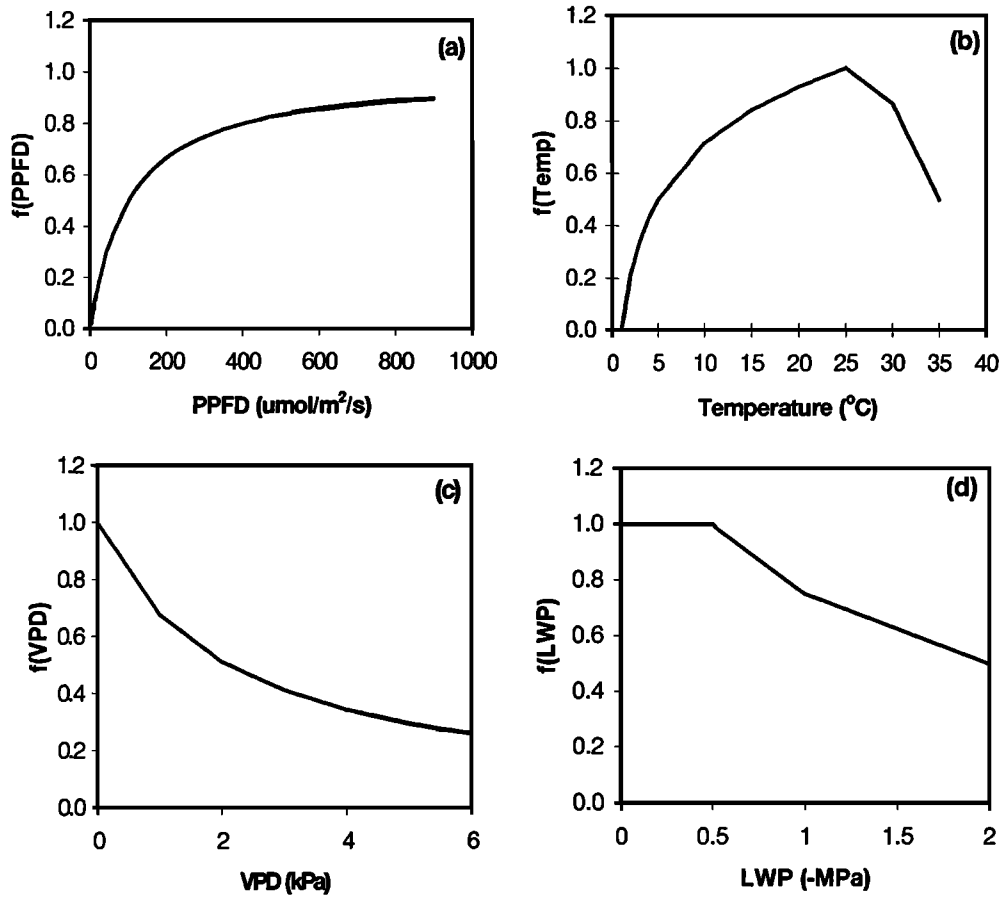

Figure 1. Stomatal response to (a) photosynthetic photon flux density (PPFD), (b) air temperature, (c) vapour pressure deficit, and (d) leaf water potential as affected by the environmental scalars ranged from 0 to 1.

sites is shown in Figure 2. The integrated daily NPP model characterized by equation (9) after sunlit and shaded leaf separation agree well with the measured values at both SOBS (Figure 2a) and SOA (Figure 2b) sites. The good agreement in both the magnitude and the day-to-day variation pattern provides evidence for the following points: (1) the method of isolating the overstory for NPP validation is effective; and (2) NPP can be estimated with a good accuracy at daily steps with consideration of general diurnal variation patterns of meteorological variables.

We have also tested two other models: (1) a big-leaf model, i.e., multiple layers of leaves are represented by a single leaf through the use of canopy conductance [*Kimball et al.*, 1997], and (2) a sunlit and shaded leaf separation model implemented at daily steps without considering the diurnal variation in meteorological variables, i.e., using the daily means for photosynthesis calculation without the daily integration in equation (9). We found that the big-leaf model could simulate the general seasonal pattern using the same leaf biochemical parameters as the integrated daily NPP model, but it missed most of the day-to-day variation found in the flux measurements. The sunlit-shaded leaf model without daily integration showed appropriate day-to-day variations in NPP but overestimated NPP by 1.5-2 times [*Chen et al.*, 1999a]. This is mostly due to the optimization of the radiation effect on photosynthesis through the use of daily mean radiation. The light saturation, which happened frequently for sunlit leaves, never occurred in such daily step calculations. This is a particularly important problem for highly clumped boreal coniferous forests [*Chen et al.*, 1999a]. We therefore selected the integrated daily NPP model for application to the BOREAS region.

4. Application of BEPS Over the BOREAS Study Region

After the above validation, BEPS was applied over the entire BOREAS study region located in Manitoba and Saskatchewan, Canada (Plate 1). The modeling domain consists of 1200 by 1200 pixels at 1 km resolution in Lambert conformal conic (LCC) projection (standard parallels, 49° N and 77° N; reference meridian, 95° W). Hudson Bay is located in the top right corner and Lake Winnipeg in the bottom right corner. The two smaller boxes designate the boundary of the southern study area (SSA) and the northern study area (NSA). The larger box outlines the boundary of the study region (SR) (see Table 3 for the geographical coordinates). The input data for BEPS are summarized in Table 4, and briefly discussed below.

4.1. Land Cover

The land cover map of the BOREAS region (Plate 1a) is part of a 1995 Canada-wide map prepared using data from

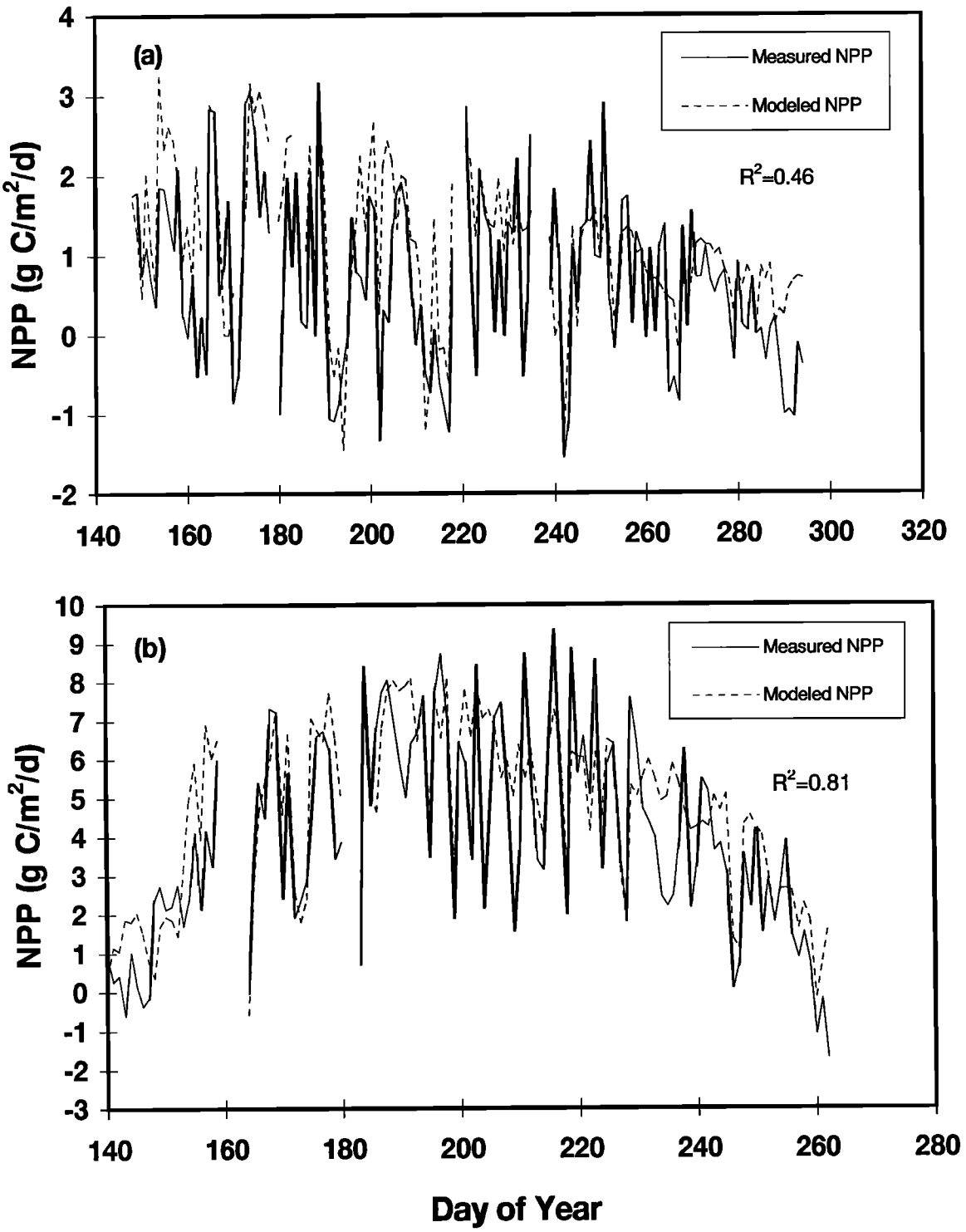

Figure 2. Daily variations in overstory net primary productivity obtained from flux measurements above and below the overstory in comparison with modeled results (a) at the old black spruce site, northern study area in 1996, and (b) at the old aspen site, southern study in 1994.

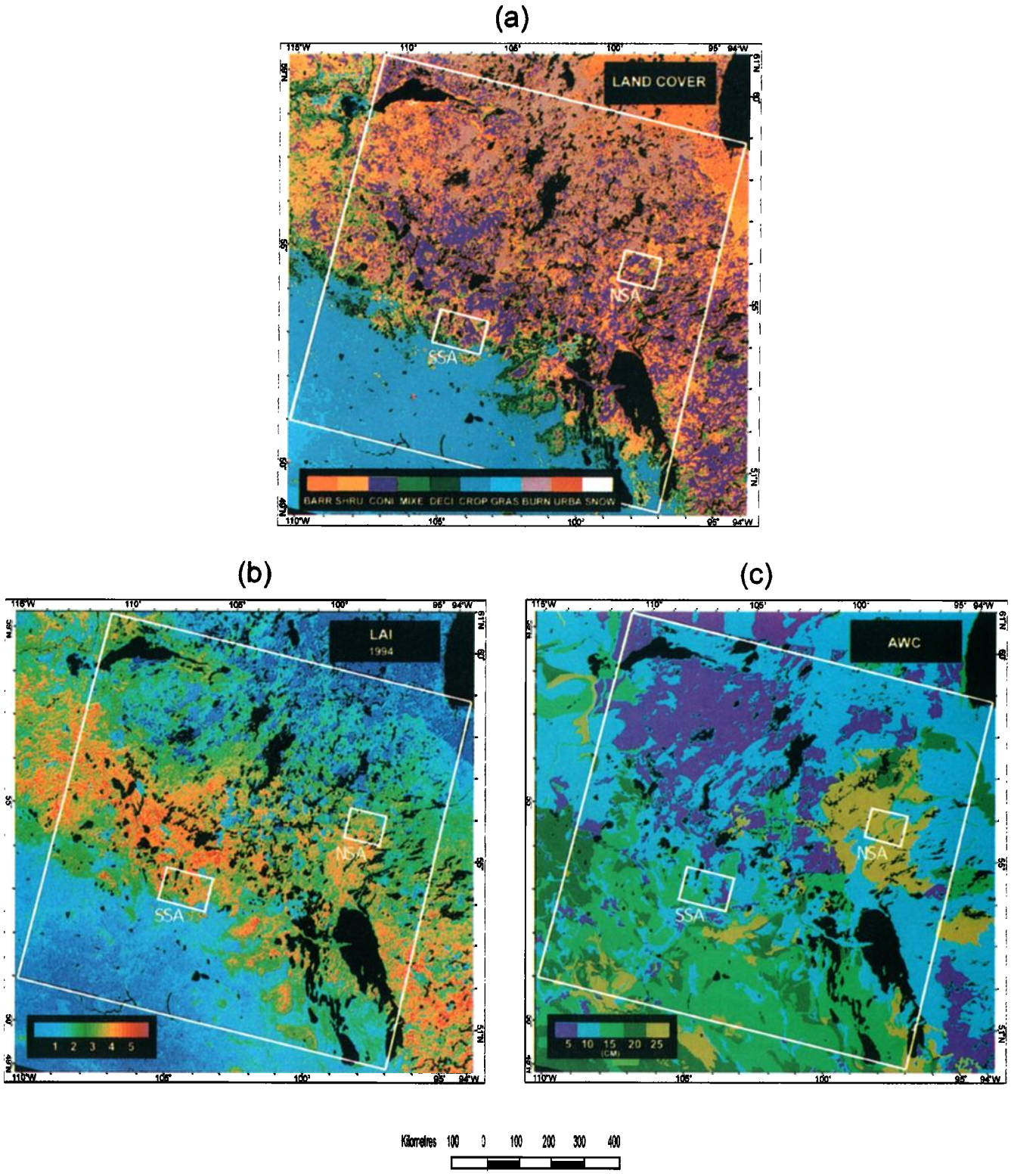

Plate 1. (a) Land cover map of the BOREAS region after *Cihlar et al.* [1997a]. BARR denotes barren land; SHRU, shrub land/wetland; CONI, coniferous forest; MIXE, mixed forest; DECI, deciduous forest; CROP, cropland; GRAS, grass land; BURN, burnt areas; URBA, urban areas; SNOW, snow/ice areas. (b) Mean leaf area index in the BOREAS region in 1994 growing season. (c) Soil available water-holding capacity in the BOREAS region.

Table 3. Coordinates of Study Area, Study Region and Image Covering the Modeling Domain

Scope	Corner	Long/Lat Coordinates		LCC Coordinates[a]	
		Longitude	Latitude	Pixel	Line
Image	NW	-115.412	59.362	0	0
	NE	- 93.286	61.010	1200	0
	SE	- 93.739	50.027	0	1200
	SW	-110.254	48.830	1200	1200
Study region	NW	-111.000	59.979	251	4
	NE	-93.502	58.844	1194	235
	SE	-96.970	50.089	970	1192
	SW	-111.000	51.000	7	954
Northern study area (NSA)	NW	-98.82	56.247	879	511
	NE	-97.24	56.081	974	534
	SE	-97.49	55.377	955	610
	SW	-99.05	55.540	860	587
Southern study area (SSA)	NW	-106.23	54.319	396	665
	NE	-104.24	54.223	520	696
	SE	-104.37	53.419	499	782
	SW	-106.32	53.513	374	751

[a]LCC is the Lambert conformal conic projection, which is the projection of the images presented in this study.

AVHRR onboard the NOAA-14 satellite. Prior to the classification, a series of data correction procedures was applied to correct the atmospheric and bidirectional reflectance effects, to remove contaminated pixels, and to determine the growing season length [*Cihlar et al.*, 1997a]. The growing-season average values in AVHRR channel 1 (C1, red), channel 2 (C2, nearinfrared) and the normalized difference vegetation index ($NDVI_m$) were then used in the classification process. A combined enhancement - unsupervised classification methodology was used [*Beaubien et al.*, this issue; *Cihlar and Beaubien*, 1998]. The resulting spectral clusters were labeled with the use of Landsat Thematic Mapper (TM) images and field observations. Accuracy was evaluated by provincial forest inventory agencies and in comparison with Landsat TM classifications. Land cover patterns in the AVHRR-derived map was found consistent with provincial maps, after allowing for the difference in scales. Numerical accuracy is variable, mainly because of the mixed land cover within AVHRR pixels [*Cihlar et al.*, 1996]. On basis of a digital comparison with Landsat Thematic Mapper classification [*Klita et al.*, 1998] the per-class accuracy varied between 21.8% and 97.9%. Detailed information on the procedure and characteristics of the AVHRR land cover map is given by *Cihlar and Beaubien* [1998].

The original classes were regrouped into 11 categories (Table 5). A pixel was labeled as deciduous if 60% of the area in the pixel was occupied by deciduous forest, whereas the pixel was classified as coniferous group if 60% of the area in the pixel was occupied by coniferous forest. Coniferous forest

Table 4. Input Data Sources and Formats

Parameter	Source	Agency[a]	Data Type	Grid System	Temporal Interval	Grid Size
LAI	AVHRR[b]	CCRS	raster	pixel/line	10 days	1 km
Land cover	AVHRR[b]	CCRS & CFS	raster	pixel/line	annual	1 km
AWC	SLC[c]	CLBRR	vector		long term	
Radiation Temperature Humidity Precipitation	NMC medium range forecast model	NCAR	raster	Gaussian	daily	~0.9° (varied with lat/long)

[a]CCRS, Canada Centre for Remote Sensing, Natural Resources Canada; CFS, Canadian Forest Service; CLBRR, Centre for Land and Biological Resources Research, Agriculture and Agri-Food Canada; NCAR, National Center for Atmospheric Research, Boulder, Colorado.
[b]Advance very high resolution radiometer.
[c]Soil Landscapes of Canada.

Table 5. Percentage of Land Cover Type in Study Region and by Study Area

Land Cover Type	Study Region		SSA		NSA	
	No. Pixel[a]	% Total	No. Pixel	% Total	No. Pixel	% Total
Coniferous forest	399080	41.3	5854	49.6	5729	71.0
Deciduous forest	29540	3.1	1027	8.7	20	0.2
Mixed forest	36037	3.7	1748	14.8	340	4.2
Cropland	202947	21.0	1412	12.0	0	0.0
Grassland	8166	0.8	8	0.1	0	0.0
Shrubland	58828	6.1	874	7.4	986	12.3
Burnt area	82319	8.5	158	1.3	72	0.9
Barren land	21038	2.2	3	0.03	164	2.0
Ice/snow	220	0.02	0	0.0	0	0.0
Urban	286	0.03	0	0.0	11	0.1
Open water	128071	13.3	728	6.2	746	9.2
Total	966532	100.0	11812	100	8068	100

Classes are based on *Cihlar et al.* [1997a] and regrouped to 11 classes (see text). SSA, the southern study area; NSA, the northern study area.
[a]1 pixel≈1 km^2.

was a dominant vegetation type in the study region and in the study areas (Table 5). Cropland occupied the second largest area in the region but not in the study areas. There were more pixels with deciduous forest in SSA than in NSA.

4.2. Leaf Area Index (LAI)

The LAI is defined here as half the total leaf area (all sides) per unit ground surface area [*Chen and Black*, 1992]. For spruce needles with four sides, for example, two sides are included in this LAI definition. For flat broad leaves with two sides, this definition is the same as the traditional definition for one-sided leaf area. LAI images in 1994 for the BOREAS region were derived from the same AVHRR sensor using 10-day cloud-free composite images [*Cihlar et al.*, 1997b]. The composites were produced using the maximum NDVI criterion and were corrected for the atmospheric and Sun-view angle effects [*Cihlar et al.*, 1997b]. The residual cloud contamination was detected from the seasonal NDVI trajectories of individual pixels and removed using a temporal interpolation scheme [*Cihlar*, 1996]. For the calculation of LAI, the NDVI was first transformed into the simple ratio (SR). Land cover specific linear SR-LAI relationships were then used to convert SR to LAI. The use of SR reduces the problem of signal saturation at high LAI values. Because the LAI of boreal vegetation is generally low and the strong foliage clumping reduces the effective LAI, no saturation was found for boreal forests when SR is used [*Chen and Cihlar*, 1996]. The algorithm for boreal coniferous forests was developed by *Chen and Cihlar* [1996]. The algorithm for deciduous forests is based on *Chen et al.* [this issue], but is less accurate because of insufficient field data for the seasonal coverage and variable understory. Mixed forest was treated as an intermediate case between coniferous and deciduous forests. An algorithm for the cropland was formulated using published relationships [*Asrar et al.*, 1984; *Aase et al.*, 1986; *Wiegand et al.*, 1992; *Li et al.*, 1993] and validated using 1996 ground measurements in 14 agricultural fields in Saskatchewan located in the lower part of the LAI image. The grassland was treated as cropland because of lack of independent measurements. To consider the effect of the seasonal greenness change in the background (understory, moss and soil/litter) of coniferous stands, a seasonal background SR trajectory was derived from AVHRR SR time series to ensure that the seasonal variation in the conifer overstory LAI was equal to or less than 25%. The formulae for the various land cover types are

$$\text{Decidous forest} \quad LAI = 0.475(SR - 2.781), \tag{17a}$$

$$\text{Coniferous forest} \quad LAI = 1.188\,(SR - B_c), \tag{17b}$$

$$\text{Mixed forest} \quad LAI = 0.592\,(SR - B_m), \tag{17c}$$

Crop land and other land cover types

$$LAI = 0.325(SR - 1.5), \tag{17d}$$

where SR is the simple ratio; B_c and B_m are background SR trajectory for coniferous forest and mixed forest. They are calculated from $B_c = 0.1(1.2X10^{-10}D^5 - 1.1X\,10^{-7}D^4 + 4.1X\,10^{-5}D^3 - 6.8X\,10^{-3}D^2 + 5.4X10^{-1}D - 15)$, and $B_m = (B_c + 2.781)/2$, where D is the day of year. The error in a single LAI value is estimated to be ±25%.

A time series of LAI images at 10-day intervals during the growing season was prepared. In a normal year, the growing season would be covered with 20 LAI images spanning from April 11to the last day of October. The LAI values before April 11 and after the last day of October were linearly interpolated between these two dates. Because of the NOAA-11 AVHRR sensor failure in September 1994, only the first 15 images were acquired by September 10 (day of year = 253). The five missing images were supplemented using measurements by the same sensor in late 1993. This might introduce some inaccuracy in the 1994 LAI values. However, the effect of LAI on NPP in the late growing season is small. Plate 1b shows the mean LAI in the growing season of 1994. The mean LAI value was 3.3 for both study areas and 2.3 for the whole study region.

4.3. Available Water-Holding Capacity (AWC)

Soil AWC data were acquired from the Soil Landscapes of Canada (SLC) database [*Shields et al.*, 1991]. SLC is compiled in a geographic information system (ARC/INFO). In SLC, the land is divided into landscape polygons within which the soils are characterized by a set of attributes. The available water holding capacity (AWC) in the upper 120 cm of soil is one of the attributes contained in SLC version 1.0. In the BOREAS region, most roots were distributed in the upper 120 cm of soil. About 10% of the area were missing data (mostly in the north) in SLC version 1.0. In order to fill in the data gaps, soil texture data in SLC version 2.0 were processed, and the dominant soil texture in each polygon was determined. AWC was then assessed according to its relationship with soil texture [*De Jong et al.*, 1984]. The AWC data in different polygons and coverages were combined, rasterized, and resampled to the same LCC projection and spatial resolution as the land cover and LAI maps. There were five levels of AWC ranging from 5 cm to 25 cm in 5 cm increments (Plate 1c). In the BOREAS region, AWC of cropland and pasture was generally higher than that of forest land. AWC of forests ranged from 5 to 10 cm except for two areas, one around the NSA with AWC of about 25 cm and the other at the forest edge close to the cropland where AWC was around 20 cm. SLC is the best soil database currently available for the country. Although polygons in the database are generally larger than 1 km, especially in the northern part of the BOREAS region, distinct spatial variation patterns are evident in Plate 1c.

4.4. Meteorological Data

Meteorological data were obtained from the National Center for Atmospheric Research (NCAR) (Table 4). The data were generated by the National Meteorological Center of NCAR from a medium range forecast model and provided in a Gaussian grid format with a grid size of about 0.9°. All meteorological data were bilinearly interpolated to each pixel at 1 km resolution [*Mather*, 1987] after determining the geographical location of the pixel in the LCC projection based on *Snyder* [1989].

On the basis of the NCAR data set, meteorological conditions over the BOREAS study region in 1994 are shown in Plate 2 and Table 6. Plate 2 displays the spatial distribution of meteorological parameters, and Table 6 provides averaged values of these parameters over the study region and the intensive study areas. The latitudinal gradient of solar radiation was evident, as were the gradients of air temperature and water vapor density (Plate 2). From the northern to the southern boundary of the study region, the mean daily radiation ranged from 9 to 11 MJ m^{-2} d^{-1}, the mean daily air temperature from –7.5° to 4.5°C, and vapor density from 4.1 to 7.4 g m^{-3}. Radiation, temperature, and vapour density were all higher in SSA than in NSA. The total annual precipitation ranged from 180 to 480 mm yr^{-1} with no obvious latitudinal gradients.

The quality of NCAR meteorological data was checked against independent measurements. The solar radiation data were compared with observations at over 40 stations in Canada. As found in an earlier study [*Liu et al.*, 1997], incident global radiation was generally overestimated by 30-40% in the NCAR data set because radiation absorption by aerosols was neglected. This overestimation was corrected with a reduction coefficient [*Liu et al.*, 1997]. The temperature and humidity of the NCAR gridded data were bilinearly interpolated to the NOBS site and checked against measurements at the top of the tower during the growing season in 1994. The mean temperature difference was found to be 0.1°C with a correlation coefficient of 0.97. The mean relative humidity measured at the tower was 17% larger than the interpolated NCAR value. The total growing season precipitation was 201 mm by NCAR but 238 mm according to rain gage measurements made at the Thompson Airport. The differences in these variables are small compared with the spatial heterogeneity, and therefore no systematic adjustments were made to the NCAR data for temperature, humidity and precipitation.

4.5. Parameterization for Calculating Plant Respiration Over the Region

Biomass and respiration coefficients are critical parameters for plant respiration calculation. Table 7 provides a list of biomass and maintenance respiration coefficients for major forest types in the region. The biomass data were assembled from *Gower et al.* [1997], *Steele et al.* [1997] and *Ryan et al.* [1997] at the tower sites. To determine the proportion of black spruce and jack pine within the conifer type, a high-resolution (30 m) land cover map [*Beaubien et al.*, this issue] was analyzed. The map is a mosaic of six Landsat Thematic Mapper scenes covering about half the study region from north to south. It was found that the conifer area consists of 18% jack pine and 82% black spruce. The biomass data from the conifer tower sites were therefore averaged, with 80% weight for black spruce and 20% for jack pine. It was assumed that the biomass data in Table 7 were representative of the region. Sapwood was estimated from stem biomass. The maintenance respiration coefficients for coniferous forest were the same as those used in BIOME-BGC [*Kimball et al.*, 1997], but only one coefficient was used for root as an intermediate value between the coefficients for fine root and coarse root. The coefficients for deciduous forest were derived from a previous study [*Liu et al.*, 1997], after adjusting for the different base temperature used in this study. Intermediate values between coniferous and deciduous forests were taken for the mixed forest type. Growth respiration coefficients were set according to *Ryan* [1991] and *Raich et al.* [1991]. For the other land cover types without biomass data, maintenance respiration was estimated using LAI [*Bonan*, 1995]; that is, instant maintenance respiration equals $LR_{f25}(1+p)2.0^{(T-25)/10}$, where L is the total leaf area index, R_{f25} is foliage respiration at 25 °C, and p is nonfoliage contribution to maintenance respiration. Both R_{f25} and p are vegetation-type-dependent and their values are given by *Bonan* [1995].

In model simulations, meteorological and biomass data were used without any adjustments to the coefficients. Adjustments are sometimes required by other process models, such as the DEMETER model [*Foley*, 1994], to confine the ratios of autotrophic respiration to GPP within a prescribed range. In our case, such adjustments were not necessary because the coefficients obtained from the various sources appear to be reliable. When using the coefficients, along with the biomass and temperature data, to calculate annual respiration rates at the tower sites, these rates were found to be generally compatible with measurements made by *Ryan et al.* [1997] and *Lavigne and Ryan* [1997].

Table 6. Meteorological Information in 1994

Parameter	Unit	Study Region			Study Area	
		Mean	Min	Max	SSA	NSA
Solar radiation	MJ m^{-2} d^{-1}	9.9	9.0	11.0	10.2	9.8
Temperature	°C	-0.5	-7.5	4.5	0.8	-1.7
Vapor density	g m^{-3}	5.9	4.1	7.4	6.1	5.3
Precipitation	mm yr^{-1}	345	180	480	334	346

Values were calculated pixel by pixel over the entire image. The values represent yearly mean for all the parameters except for precipitation, which is yearly total. For the study areas, mean value over each of the area is listed, while for the study region, maximum (max) and minimum (min) in the region are added.

5. Result and Discussion

5.1. NPP Distribution Over the BOREAS Region

The distribution of NPP over the BOREAS region in 1994 is shown in Plate 3. The most productive area was the forest, which appears as a wide strip oriented in the northwest-southeast direction in the middle of the region. The average NPP in SSA, located near the southern border of the boreal forest zone, was higher than that in NSA located near the northern limit of the zone. The average NPP in the study region was lower than that of both study areas (Table 8). Deciduous forests showed the highest photosynthetic capacity among all vegetation types. The average NPP values for coniferous and deciduous forests in the study areas are close to the values for the tower flux sites reported by *Gower et al.* [1997] and *Ryan et al.* [1997] but are higher than those modeled by *Frolking* [1997] and *Kimball et al.* [1997]. The range in NPP between these two study areas was smaller for coniferous forest, and larger for deciduous forest than the measurements reported by *Gower et al.* [1997] and *Ryan et al.* [1997]. These differences between site averages and the regional averages underscore the importance of explicitly accounting for the spatial heterogeneity.

The mean NPP over the study region was calculated to be 217 g C m^{-2} yr^{-1} in 1994 (Table 8). This average, which excludes open water pixels, is highly influenced by the land cover composition. The mean NPP of all forests, excluding burnt areas, was 234 g C m^{-2} yr^{1}, providing a better overall measure of forest productivity. The total NPP in the 1000 km x 1000 km study region was estimated to be182 Mt C in 1994 (Table 9). The largest proportion was attributed to the coniferous forest because of its dominant presence in the region. Cropland was the second largest contributor, while deciduous and mixed wood forests contributed about 15% to total NPP.

5.2. Gross Primary Productivity (GPP) and Plant Respiration

As shown in Table 10, GPP in NSA was lower than that in SSA, while GPP in the study region was lower than those in both study areas. Deciduous forests had higher GPP than coniferous forests within the same area. The GPP value for cropland was lower than that of coniferous forests in SSA but higher than that of coniferous forests in NSA. The spatial distribution of autotrophic respiration followed a pattern similar to GPP for the major vegetation types in the study region.

5.3. Relationships Between NPP and LAI

In the BOREAS region, NPP was strongly correlated to LAI, as shown in Figure 3. The data points were sampled at regular intervals within the study region at rates of 1% for coniferous forests and cropland and 10% for deciduous forests. NPP was approximately linearly related to LAI when LAI was below 4 and became asymptotic (saturated) as LAI increased further. This saturation occurs because the increase in canopy radiation absorption with LAI becomes small at large LAI values. This saturation was more apparent in conifers than in other vegetation types. Good relationships between aircraft-measured downward CO_2 flux and vegetation indices, such as the NDVI and greenness index, were also found in other studies [*Cihlar et al.*, 1992; *Ogunjemiyo et al.*, 1997], suggesting that productivity is closely related to LAI at large scales. *Gower et al.* [1997] reported that only conifers followed a relationship between aboveground NPP and overstory LAI, although most LAI values in their report were above 4. At the same LAI value, deciduous forests showed higher productivity than coniferous forests, confirming the importance of land cover information in NPP modeling based on LAI distributions. *Gower et al.* [1997] also observed a

Table 7. Maintenance Respiration Coefficients and Carbon Contents for Various Forests

Parameters	Unit	Coniferous Forest	Deciduous Forest	Mixed Forest
Leaf respiration coefficient	kg C d^{-1} kg^{-1}	0.002	0.009	0.006
Stem respiration coefficient	kg C d^{-1} kg^{-1}	0.001	0.005	0.003
Root respiration coefficient	kg C d^{-1} kg^{-1}	0.0015	0.0015	0.0015
Leaf carbon	kg C m^{-2}	0.6	0.1	0.4
Stem carbon	kg C m^{-2}	5.1	7.3	4.2
Root carbon	kg C m^{-2}	1.2	1.3	1.2

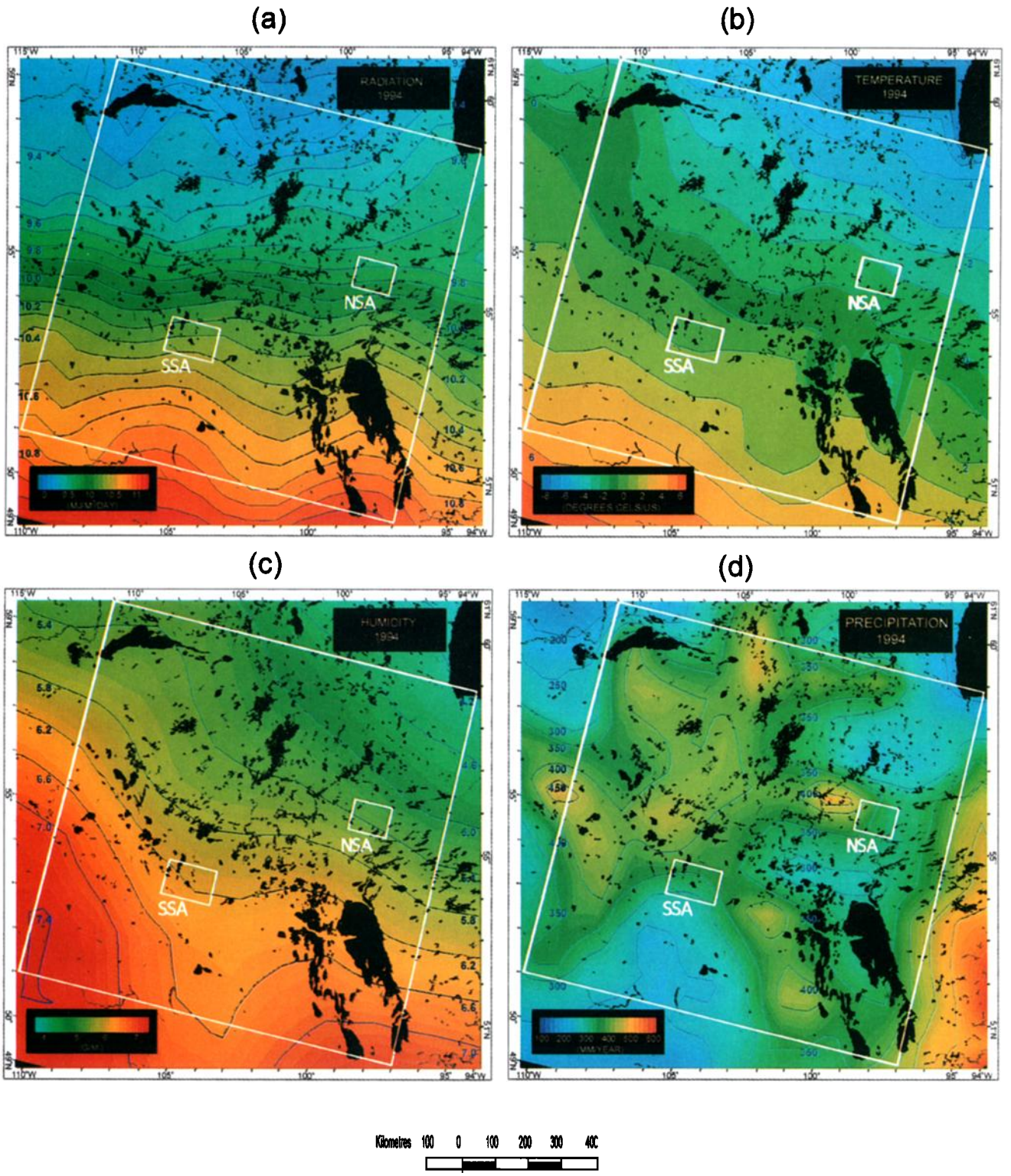

Plate 2. Distribution of meteorological parameters in the BOREAS region in 1994. (a) Mean daily total shortwave radiation (MJ m^{-2} d^{-1}). (b) Mean daily air temperature (°C). (c) Mean daily water vapor density (g m^{-3}). (d) Yearly total precipitation (mm yr^{-1}).

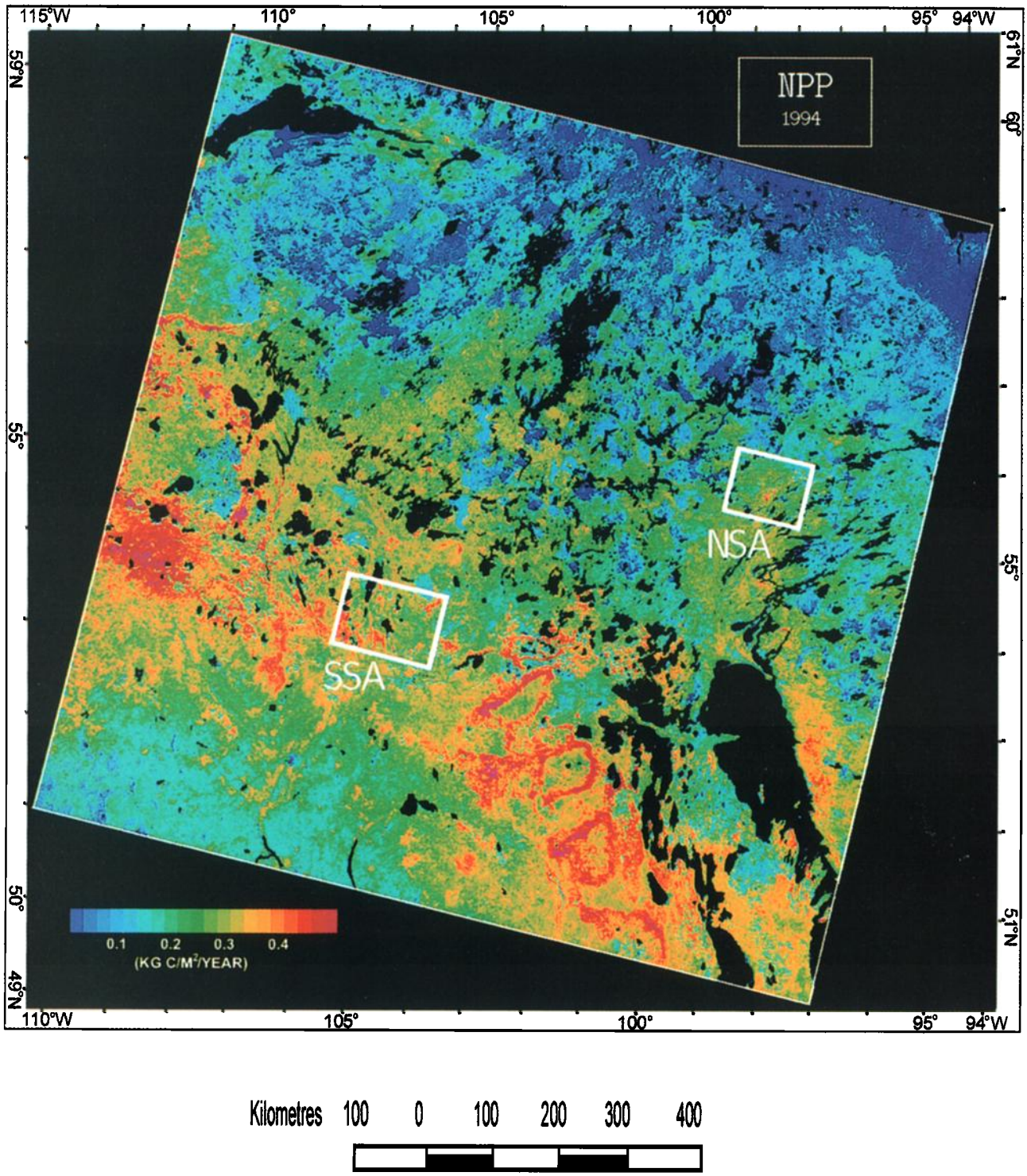

Plate 3. Net primary productivity over the BOREAS region in 1994.

Table 8. BEPS Estimates of Mean NPP of Major Vegetation Types, Forest, and Land in BOREAS Study Region and Study Areas in 1994 (g C m^{-2} yr^{-1})

Land Cover Type	Study region		SSA		NSA	
	Mean	s.d.	Mean	s.d.	Mean	s.d.
Coniferous forest	207	92	276	55	247	57
Deciduous forest	418	91	395	92	283	75
Crop	284	80	312	58		
Forest	234	113	308	82	253	61
Land	217	122	297	86	238	76

"Forest" refers to all forest pixels, including coniferous forest, deciduous forest, and mixed forest in Table 5. "Land" refers to all land pixels, excluding water body. s.d., standard deviation.

Table 9. Total NPP in BOREAS Study Region in 1994

Land Cover Type	Number of Pixel[a]	Class Mean NPP (g C m^{-2} yr^{-1})	Class Total NPP (Mt C yr^{-1})
Coniferous forest	399080	207	83
Deciduous forest	29540	418	12
Mixed forest	36037	380	14
Cropland	202947	284	58
Grassland	8166	109	1
Shrubland	58828	175	10
Burnt area	82319	44	4
Barren land	21038	20	0
Ice/snow	220	0	0
Urban	286	62	0
Open water	128071	0	0
Total	966532		182

[a]1 pixel≈1 km^2.

Table 10. Mean GPP and Autotrophic Respiration of Major Vegetation Types, Forest and Land in BOREAS Study Region and The Study Areas in 1994

Land Cover Type	GPP (g C m^{-2} yr^{-1})			R_{auto} (g C m^{-2} yr^{-1})		
	Study Region	SSA	NSA	Study Region	SSA	NSA
Coniferous forest	614	757	677	406	480	428
Deciduous forest	967	931	727	548	534	442
Crop	669	706		383	392	
Forest	660	808	686	425	499	432
Land	583	767	646	365	469	406

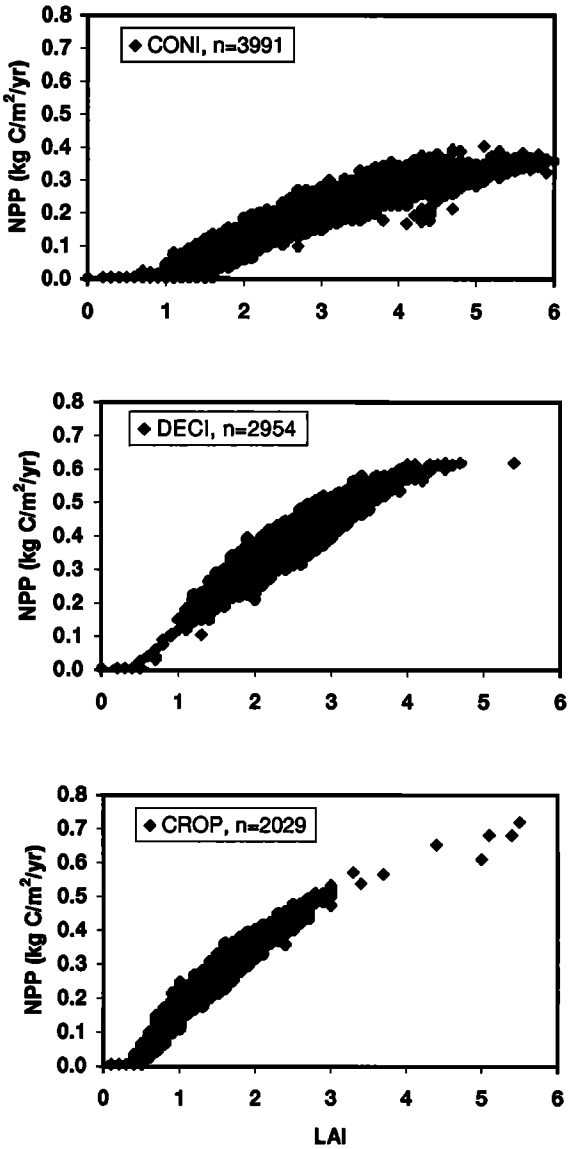

Figure 3. Relationships between net primary productivity (NPP) and leaf area index (LAI) for the three major cover types: deciduous, conifer and cropland.

higher production efficiency, expressed as the ratio of aboveground NPP to LAI, for aspen than for coniferous forests.

In spite of the general relationship between NPP and LAI, large variations of NPP existed for a given LAI (Figure 3). These variations resulted from different vegetation, weather, and soil conditions. The variation may be larger in areas with more topographical variation than the BOREAS region. Although the relationship between NPP and LAI can be generally expressed by quadratic equations for different land cover types, the coefficients determining shape of a curve would vary from region to region and from year to year under different the climatic and environmental conditions. These coefficients are difficult to determine using empirical approaches, underscoring the importance of using a process model in integrating remote sensing, soil, and meteorological data for regional NPP estimation.

5.4. Relationships Between Forest NPP and Environmental Conditions

To briefly examine the influence of environmental conditions on forest NPP, the NPP values at LAI between 2 and 3 were sampled over the study region at a rate of 10% for coniferous forest and 100% for deciduous forest. Environmental parameters were also sampled for the same pixels, including absorbed photosynthetically active radiation (APAR), air temperature, vapor pressure deficit (VPD), precipitation, and available water holding capacity. The correlation coefficients (R) between NPP and each environmental parameter are listed in Table 11. NPP was highly correlated with APAR, especially for deciduous forest. *Chen et al.* [1999b] also found that APAR was a major factor controlling the photosynthetic rate at the SOA site. By contrast, correlation between NPP and the incoming radiation was weak. This result shows the importance of LAI to NPP because APAR is dependent on both incoming radiation and LAI. An increase in temperature has three effects: (1) enhancing photosynthesis when the temperature is below the optimal point but decreasing photosynthesis otherwise (Figure 1b), (2) increasing plant respiration (equation (12)), and (3) increasing VPD at a given vapor density. It appears that the overall effect resulted in a negative correlation between temperature and NPP for the forest types in the region for 1994. It is difficult to isolate the effect of temperature from VPD because they are strongly correlated. The correlation coefficient between temperature and VPD was 0.69 and 0.81 for coniferous forest and deciduous forest, respectively. The negative effect of VPD agrees with that reported by *Dang et al.* [1997]. Deciduous forest was more sensitive to VPD than coniferous forest. Soil water might not be a limiting factor in the region, as indicated by the low coefficients associated with precipitation and soil water holding capacity. However, the positive sign of the coefficients suggests some benefit of sufficient soil water to plant growth.

5.5. Light use efficiency (LUE or ε) in the BOREAS Region

Light use efficiency (ε) [*Monteith*, 1972], refers to the ratio of energy output (in terms of carbohydrate or dry matter) to energy input (in terms of absorbed solar radiation). For the calculation of light use efficiency, APAR needs to be determined from the incident radiation and the canopy architectural parameters. NPP and GPP values calculated using BEPS provide an independent means to assess ε.

Table 12 summarizes the mean light use efficiencies for NPP (ε_{NPP}) and GPP (ε_{GPP}), for the major land cover types, the study areas, and the region. Also shown is APAR during the growing season calculated from daily total solar radiation, solar zenith angle at noon, LAI, and clumping index using the methodology of *Liu et al.* [1997]. In general, ε_{GPP} was less scattered than ε_{NPP}, as indicated by the coefficient of variation. This was also observed by *Goetz and Prince* [1998]. In recognition of this fact, ε_{GPP}, rather than ε_{NPP}, has recently been more widely used for NPP modeling in some LUE models [*Prince and Goward*, 1995; *Ruimy et al.*, 1996; *Goetz and Prince*, 1999]. In addition, large differences existed between cover types, with ε_{GPP} and ε_{NPP} about 1.5-2 times higher for deciduous than for coniferous forests (Table 12). In comparison with ε_{NPP} calculated by *Hunt and Running* [1992] in the same area, the values in Table 12 are considerably

Table 11. Correlation Coefficients (R) between Forest NPP and Environmental Parameters

Forest Type	APAR	TEM	VPD	PRE	AWC
Coniferous forest	0.79	-0.06	-0.28	0.03	0.12
Deciduous forest	0.82	-0.33	-0.37	0.24	0.10

APAR, absorbed photosynthetically active radiation; TEM, temperature; VPD, vapour pressrure deficit; PRE, precipitation; AWC, available water holding capacity.

smaller, but they are more consistent with the estimates from *Gower et al.* [1998], who reported the values around 0.3 g C MJ^{-1} for black spruce and jack pine. From measurements made in several tens of stands in northeast Minnesota, *Goetz and Prince* [1996] reported the mean values of ε_{NPP} of aspen and black spruce to be 0.45 g C MJ^{-1} and 0.24 g C MJ^{-1}, respectively. These values are slightly larger than the corresponding values reported in Table 12. The ε values for crop were lower than those in Britain and the United States (ε_{NPP} = 0.5~ 2 g C MJ^{-1}) [*Monteith*, 1977; *Kiniry et al.* 1989] but higher than the global average for ε_{NPP} (=0.242 g C MJ^{-1}) [*Potter et al.*, 1993] and ε_{GPP} (=0.41 g C MJ^{-1}) [*Prince and Goward*, 1995].

5.6. Possible Sources of Errors and Directions for Improvements

Although considerable efforts have been made to minimize the uncertainties in NPP estimation over the BOREAS region, some sources of error inevitably remain. They include within-pixel heterogeneity, simplification of natural processes with a daily photosynthesis model, errors in meteorological and soil input data, assignment of biological parameters for the various cover types, and the accuracy of image registration and processing (resampling, radiance-to-reflectance conversion, etc). Because of the additive effects of these sources of errors, the NPP values for individual pixels can be as large as 25-50%. However, since the model parameters and the final NPP results have been carefully calibrated using tower flux data, the major bias errors are much reduced, and therefore the errors in the regional NPP estimates are expected to be smaller than 25%. Many of these sources of error are presently inherent in large area applications. There are several ways to improve the accuracy of the estimation.

5.6.1 Consideration of subpixel heterogeneity using high-resolution remote sensing data. *Chen* [1999] showed that the largest errors of this type result from mixed water and land pixels and a large improvement can be made by just using the information of sub-pixel water area fraction.

5.6.2 Improving the biomass data quality. We expect that the NPP spatial distribution pattern would be more accurate if a remotely derived biomass map were used rather than assigning the value by cover type. The feasibility of estimating biomass distribution from active microwave images has been demonstrated [*Moghaddam et al.*, 1994]. Optical measurements can also be useful for this purpose for sparse canopies [*Hall et al.*, 1995].

5.6.3 Reducing the computation time step. Although the problem associated with diurnal variability is much smaller when using the integrated daily NPP model, errors are still inevitable in the daily step calculations which cannot capture subdaily extreme events [*Chen et al.*, 1999a]. With the improvement in computational capacity, it will soon be feasible to compute a moderate-resolution NPP distribution in a region at much smaller time steps (minutes to hours). Such work is only possible in conjunction with a global circulation model to avoid data limitation.

6. Summary

For the purpose of studying the carbon cycle in boreal ecosystems, the spatial distribution of net primary productivity (NPP) in the BOREAS region was derived by integrating tower-based and other ground measurements with remote sensing images. The major characteristics of the resulting NPP map are as follows:

1. NPP is calculated using a process model, with a new daily integration scheme through an analytical integration of Farqhuar's photosynthesis model. The model is more complex than the original Farqhuar model, but it requires no additional parameters and is computationally efficient as well as numerically stable. Nonlinear effects of meteorological variables on productivity within the daily step are therefore much reduced through the analytical daily integration considering the general diurnal patterns of the variables.

Table 12. Light Use Efficiency for NPP (ε_{NPP}) and GPP (ε_{GPP}) by Major Vegetation Type and by Area Covered

	ε_{NPP} (g C (MJ APAR)$^{-1}$)			ε_{GPP} (g C (MJ APAR)$^{-1}$)			APAR (MJ m^{-2})	
	Mean	s.d.	CV (%)	Mean	s.d.	CV (%)	Mean	s.d.
Land cover type								
coniferous forest	0.20	0.07	36	0.60	0.09	14	1002	133
deciduous forest	0.40	0.07	16	0.93	0.06	6	1042	79
crop	0.33	0.06	17	0.76	0.15	20	863	119
Area covered								
study region	0.22	0.12	52	0.61	0.22	36	927	164
SSA	0.28	0.08	29	0.72	0.14	19	1059	120
NSA	0.22	0.06	27	0.62	0.13	21	1036	113

CV, coefficient of variation.

2. Simultaneous tower measurements of CO_2 fluxes above and below the overstory canopy at a coniferous site and a deciduous site were used to validate the daily NPP model. A method was developed to isolate the overstory for daily NPP validation. The productivity of the understory (shrubs, grass, and moss) is therefore not included in the NPP.

3. The process model is implemented over the BOREAS regio through the use of remote sensing data that provide spatial distributions of leaf area index and land cover type. Therefore the effects of canopy architecture on radiation absorption and on productivity are considered explicitly. With the use of land cover information, the physiological differences among the major boreal forest types are also considered.

Notation

A net photosynthesis rate, μmol m^{-2} s^{-1}.

A_c Rubisco-limited net photosynthesis rate, μmol m^{-2} s^{-1}.

A_j light limited net photosynthesis rate, μmol m^{-2} s^{-1}

C irradiance from multiple scattering of direct radiation, W m^{-2}.

C_i intercellular CO_2 concentration , Pa.

C_a CO_2 concentration in the atmosphere , Pa.

D day of year.

g total conductance to CO_2 from cell to air, μmol m^{-2} s^1 Pa^{-1}.

g_n conductance at noon, μmol m^{-2} s^1 Pa^{-1}.

g_s stomatal conductance to CO_2, m s^{-1}.

$g_{s,max}$ maximum stomatal conductance to CO_2, m s^{-1}.

J electron transport rate, μmol m^{-2} s^{-1}.

J_{max} light saturated rate of electron transport, μmol m^{-2} s^{-1}.

K function of enzyme kinetics, Pa.

LAI leaf area index.

LAI_{Sun} sunlit leaf area index.

LAI_{shade} shaded leaf area index.

O_2 intercellular O_2 concentration (≈21,000), Pa.

PPFD photosynthetically active flux density, μmol m^{-2} s^{-1}.

M_i biomass (or sapwood for stems) of a plant component i, kg C m^{-2}.

N foliage nitrogen concentration, %.

N_m maximum foliage nitrogen concentration, %.

P atmospheric pressure (≈100,000), Pa.

R_a autotropic respiration, g C m^{-2} d^{-1}.

R_d daytime leaf dark respiration, μmol m^{-2} s^{-1}.

R_{gas} molar gas constant (= 8.3143), m^3 Pa mol^{-1} K^{-1}.

R_m plant maintenance respiration, g C m^{-2} d^{-1}.

R_g plant growth respiration, g C m^{-2} d^{-1}.

$r_{a,i}$ carbon allocation fraction for plant component i.

$r_{m,i}$ maintenance respiration coefficient for plant component i, kg C kg^{-1} d^{-1}.

$r_{g,i}$ growth respiration coefficient for plant component i, kg C kg^{-1} d^{-1}.

S_{dir} direct solar irradiance, W m^{-2}.

S_{dif} diffuse solar irradiance, W m^{-2}.

$S_{dif,under}$ diffuse solar irradiance under plant canopy, W m^{-2}.

S_g global solar irradiance, W m^{-2}.

S_o solar constant (=1360), W m^{-2}.

S_{sun} sunlit-leaf irradiance, W m^{-2}.

S_{shade} shaded leaf irradiance, W m^{-2}.

T air temperature, °C.

V_m maximum carboxylation rate, μmol m^{-2} s^{-1}.

$V_{m,25}$ maximum carboxylation rate at 25 °C, μmol m^{-2} s^{-1}.

W_c Rubisco-limited gross photosynthesis rate, μmol m^{-2} s^{-1}.

W_j light-limited gross photosynthesis rate, μmol m^{-2} s^{-1}.

α mean leaf-Sun angle (=60 ° for a canopy with spherical leaf angle distribution).

Γ CO_2 compensation point in the absence of dark respiration, Pa.

θ solar zenith angle, °.

θ_n solar zenith angle at noon, °.

$\bar{\theta}$ representative zenith angle for diffuse radiation transmission, °.

φ latitude of a location, °.

Ω foliage-clumping index.

Acknowledgments. The authors are grateful to T. A. Black of the University of British Columbia and M. Goulden of the University of California at Irvine for the permission to use the data for model validation. We thank Rasim Latifovic for his help in compiling soil data. Mike Sarich was very helpful in tower and remote sensing data processing and analysis. David Fraser, Goran Pavlic, Doug Eagle, and Karen McEwen provided assistance in different phases of the study. Robert Fraser and Sylvain Leblanc carefully reviewed the manuscript. We are especially grateful to C. Potter of NASA, S. J. Goetz of the University of Maryland, and an anonymous reviewer for their valuable comments. This study is part of the Northern Biosphere Observation and Modelling Experiment (NBIOME).

References

Aase, J. K., J. P. Millard, and B. S. Brown, Spectral radiance estimates of leaf area and leaf phytomass of small grains and native vegetation, *IEEE Trans. Geosci. Remote Sens., 24*, 685-692, 1986.

Asrar, G., M. Fuchs, E. T. Kanemasu, and J. H. Hatfield, Estimating absorbed photosynthetic radiation and leaf area index from spectral reflectance in wheat, *Agron. J., 76*, 300-306, 1984.

Baldocchi, D. D., B. B. Hichs, and P. Camara, A canopy stomatal resistance model for gaseous deposition to vegetated surfaces, *Atmos. Environ., 21*, 91-101, 1987.

Beaubien, J., J. Cihlar, G. Simard, and R. Latifovic, Land cover from multiple Thematic Mapper scenes using a new enhancement - classification methodology, *J. Geophys. Res.*, this issue.

Black, T.A., J. M. Chen, X. Lee, and R. M. Sagar, Characteristics of shortwave and longwave irradiances under a Douglas-fir forest stand, *Can. J. For. Res., 12*, 1020-1028, 1991.

Black, T.A., et al., Annual cycle of water vapour and carbon dioxide fluxes in and above a boreal aspen forest, *Global Change Biol.*, *2*, 101-111, 1996.

Bonan, G.B., Land-atmosphere CO_2 exchange simulated by a land surface process model coupled to an atmospheric general circulation model, *J. Geophys. Res.*, *100*, 2817-2831, 1995.

Chen, J. M., Spatial scaling of a remotely sensed surface parameter by contexture, *Remote Sen. Environ.*, in press, 1999.

Chen, J. M., and T. A. Black, Defining leaf area index for non-flat l eaves, *Plant Cell Envrion.*, *15*, 421-429, 1992.

Chen, J. M., and J. Cihlar, Retrieving leaf area index of boreal conifer forests using Landsat TM images, *Remote Sens. Environ.*, *55*, 153-162, 1996.

Chen, J. M., J. Liu, J. Cihlar, and M. L. Goulden, Daily canopy photosynthesis model through temporal and spatial scaling for remote sensing applications, *Ecol. Mod.*, in press, 1999a.

Chen, W.J., T. A. Black, P. C. Yang, A. G. Barr, H. H. Neumann, Z. Nesic, M. D. Novak, J. Eley, and R. Cuenca, Effects of climate variability on the annual carbon sequestration by a boreal aspen forest, *Global Change Biol.*, *5*, 41-53, 1999b.

Chen, J. M., S. G. Leblanc, J. R. Miller, J. Freemantle, S. E. Loechel, C. L. Walthall, K. A. Innanen, and H. P. White, Compact airborne spectrographic imager (CASI) used for mapping biophysical parameters of boreal forests, *J. Geophys. Res.*, this issue.

Cihlar, J., Identification of contaminated pixels in AVHRR composite images for studies of land biosphere, *Remote Sens. Environ.*, *56*, 149-163, 1996.

Cihlar, J., and J. Beaubien, Land Cover of Canada 1995 Version 1.1, Digital data set documentation, Natural Resources Canada, Ottawa, Ontario, http: //www.ccrs.nrcan.gc.ca /ccrs /comvnts /rsic /rsicinde.html, 1998.

Cihlar, J., P. H. Caramori, P. H. Schuepp, and R. L. Desjardins, Relationship between satellite-derived vegetation indices and aircraft-based CO_2 measurements, *J. Geophys. Res.*, *97*, 18515-18521, 1992.

Cihlar, J., H. Ly, and Q. Xiao, Land cover classification with AVHRR multichannel composites in northern environments, *Remote Sens. Environ.*, *58*, 36-51, 1996.

Cihlar, J., J. Beaubien, Q. Xiao, J. Chen, and Z. Li, Land cover of the BOREAS region form AVHRR and Landsat data, *Can. J. Remote Sens.*, *23*, 164-175, 1997a.

Cihlar, J., H. Ly, Z. Li, J. M. Chen, H. Pokrant, and F. Huang, Multitemporal, multichannel AVHRR data sets for land biosphere studies: Artifacts and corrections, *Remote Sens. Environ.*, *60*, 35-57, 1997b.

Collatz, G. J., J. T. Ball, C. Crivet, and J. A. Berry, Physiological and environmental regulation of stomatal conductance, photosynthesis and transpiration: A model that includes a laminar boundary layer, *Agric. For. Meteor.*, *54*, 107-136, 1991.

Dang, Q. L., H. A. Margolis, M. R. Coyea, M. Sy, and G. J. Collatz, Regulation of branch-level gas exchange of boreal trees: Roles of shoot water potential and vapour pressure difference, *Tree Physiol.*, *17*, 521-535, 1997.

De Jong, R., J. A. Shields, and W. K. Sly, Estimated soil water reserves applicable to a wheat-fallow rotation for generalized soil areas mapped in southern Saskatchewan, *Can. J. Soil Sci.*, *64*, 667-680, 1984.

Denning, S. A., G. J. Collatz, C. Zhang, D. A. Randall, J. A. Berry, P. J. Sellers, G. D. Colello, and D. A. Dazlich, Simulation of terrestrial carbon metabolism and atmospheric CO in a general circulation model, 1, Surface carbon fluxes, *Tellus*, Ser. B., *48*, 521-542, 1996.

Erbs, D. G., S. A. Klein, and J. A. Duffie, Estimation of diffuse radiation fraction for hourly, daily and monthly-average global radiation, *Sol. Energy*, *28*, 293-304, 1982.

Farquhar, G.D., and S. von Caemmerer, Modelling of photosynthetic response to environmental conditions, in *Encyclopedia of Plant Physiology*, new series, vol. 12B, *Physiological Plant Ecology II*, edited by O. L. Lange, P. S. Nobel, C. B. Osmond, and H. Ziegler, pp. 549-587, Springer-Verlag, New York, 1982.

Farquhar, G.D., S. von Caemmerer, and J.A. Berry, A biochemical model of photosynthetic CO_2 assimilation in leaves of C_3 species, *Planta*, *149*, 78-90, 1980.

Foley, J. A., Net primary productivity in the terrestrial biosphere: The application of a global model, *J. Geophys. Res.*, *99*, 20,773-20,783, 1994.

Foley, J. A, I. C. Prentice, N. Ramankutty, S. Levis, D. Pollard, S. Sitch, and A. Haxeltine, An integrated biosphere model of land surface processes, terrestrial carbon balance and vegetation dynamics, *Global Biogeochem. Cycles*, *10*, 603-628, 1996.

Frolking, S., Sensitivity of spruce/moss boreal forest net ecosystem productivity to seasonal anomalies in weather, *J. Geogr. Res.*, *102*, 29053-29064, 1997.

Goetz, S. J., and S. D. Prince, Remote sensing of net primary production in boreal forest stands, *Agric. For. Meteorol.*, *78*, 149-179, 1996.

Goetz, S. J., and S. D. Prince, Variability in light utilization among boreal forest stands and implications for remote sensing of net primary production, *Can. J. For. Res. 28*, 375-389,1998.

Goetz, S. J., and S. D. Prince, Modeling terrestrial carbon exchange and storage: Evidence and implications of functional convergence in light-use efficiency, *Adv. Ecol. Res.*, *28*, 57-92, 1999.

Goetz, S. J., S. D. Prince, S. N. Goward, M. M. Thawley, J. Small, and A. Johnston, Mapping net primary production and related biophysical variables with remote sensing: Application to the BOREAS region, *J. Geophys. Res. this issue.*

Goulden, M. L., and P. M. Crill, Automated measurement of CO_2 exchange at the moss surface of a black spruce forest, *Tree Physiol.*, *17*, 537-542, 1997.

Goulden, M. L., B. C. Daube, S. M. Fan, D. J. Sutton, A. Bazzaz, J. W. Munger, and S. C. Wofsy, Physiological responses of a black spruce forest to weather, *J. Geophys. Res. 102*, 28,987-28,996, 1997.

Gower, S. T., J. G. Vogel, J. M. Norman, C. J. Kucharik, S. J. Steele, and T. K. Stow, Carbon distribution and aboveground net primary productivity in aspen, jack pine, and black spruce stands in Saskatchewan and Manitoba, Canada, *J. Geophys. Res.*, *102*, 29,029-29,041, 1997.

Gower, S. T., C. J. Kucharik, and J. M. Norman, Direct and indirect estimate of leaf area index, f_{par} and net primary production of terrestrial ecosystems, *Remote Sens. Environ., in press*, 1998.

Hall, F. G., Y. E. Shimabukuro, and K. F. Huemmrich, Remote sensing of forest biophysical structure using mixture decomposition and geometric reflectance models, *Ecol. Appl.*, *5*, 993-1013, 1995.

Hunt, E. R. Jr., and S. W. Running, Simulated dry matter yields for aspen and spruce stand in the North American Boreal Forest, *Can. J. Remote Sen.*, *18*, 126-133, 1992.

Jarvis, P. G., The interpretation of the variations in leaf water potential and stomatal conductance found in canopies in the field, *Philos. Trans. R. Soc. London*, Ser. *B*, *273*, 593-610, 1976.

Jarvis, P. G., and J. I. L. Morison, Stomatal control of transpiration and photosynthesis, in "*Stomatal Physiology*," P. G. Jarvis and T. A. Mansfield (Eds.), pp. 247-279, Cambridge Univ. Press, New York, 1981.

Kimball, J. S., P. E. Thornton, M. A. White, and S. W. Running, Simulating forest productivity and surface-atmosphere carbon exchange in the BOREAS study region, *Tree Physiol.*, *17*, 589-599, 1997.

Kiniry, J. R., C. A. Jones, J. C. O'Toole, R. Blanchet, M. Cabelgue, and D. A. Spanel, Radiation use efficiency in biomass accumulation prior to grain filling for five grain field crops species, *Field Crop Res.*, *20*, 51-64, 1989.

Klita, D.L., R. J. Hall, J. Cihlar, J. Beaubien, K. Dutchak, R. Nesby, J. Drieman, R. Usher, and T. Perrott, A comparison between two satellite-based land cover classification programs for a boreal forest region in northwest Alberta, Canada, in paper presented at the 20th Canadian Symposium on Remote Sensing, CRSS and ERIM International, Inc. May 1998.

Lavigne, M. B., and M. G. Ryan, Growth and maintenance respiration rates of aspen, black spruce and jack pine stems at northern and southern BOREAS sites, *Tree Physiol.*, *17*, 543-551, 1997.

Li, Y., T. H. Demetriades-Shah, E. T. Kanemasu, J. K. Shultis, and M. B. Kirkham. Use of second derivatives of canopy reflectance for monitoring prairie vegetation over different soil backgrounds, *Remote Sens. Environ.*, *44*, 81-87, 1993.

Liu J., J.M. Chen, J. Cihlar, and W.M. Park, A process-based boreal ecosystem productivity simulator using remote sensing inputs, *Remote Sens. Environ.*, *62*,158-175, 1997.

Mather, P. M. *Computer Processing of Remotely-Sensed Images: An Introduction*, John Wiley, New York, 1987.

Melillo, J. M., and VEMAP members, Vegetation/ecosystem modeling and analysis project: Comparing biogeography and biogeochemistry models in a continental-scale study of terrestrial ecosystem responses to climate changes and CO_2 doubling, *Global Biogeochem. Cycles, 9*, 407-437, 1995.

Moghaddam, M., S. Durden, and H. Zebker, Radar measurement of forested areas during OTTER, *Remote Sens. Environ., 47*, 154-166, 1994.

Monteith, J. L., Solar radiation and productivity in tropical ecosystem, *J. Appl. Ecol., 9*, 747-766, 1972.

Monteith, J. L., Climate and the efficiency of crop production in Britain, *Philos. Trans. R. Soc. London*, B, *281*, 277-294, 1977.

Norman, J. M. Simulation of microclimates, in *Biometeorology in integrated pest management*, edited by J. L. Hatfield and I. J. Thomason, p. 65-99, Academic, New York, 1982.

Ogunjemiyo, S., P. H. Schuepp, J. I. MacPherson, and R. L. Desjardins, Analysis of flux maps versus surface characteristics from Twin Otter grid flights in BOREAS in 1994, *J. Geophys. Res., 102*, 29,135-29,145, 1997.

Oke, T. R., *Boundary Layer Climates*, 2nd ed., Routledge, New York, 1990.

Potter, C. S., J. T. Randerson, C. B. Field, and P. A. Matson, P. M. Vitousek, H. A. Mooney, and S. A. Klooster, Terrestrial ecosystem production: A process model based on global satellite and surface data, *Global Biogeochem. Cycles, 7*, 811-841, 1993.

Prince, S. D., and S. N. Goward, Global primary production: A remote sensing approach, *J. Biogeogr., 22*, 815-835, 1995.

Raich, J. W., E. B. Pastetter, J. M. Melillo, D. W. Kicklighter, P. A. Grace, B. Moore III, and B. J. Peterson, Potential net primary productivity in South America: Application of a global model, *Ecol. Appl., 1*, 399-429, 1991.

Ruimy, A., B. Saugier, and G. Dedieu, Methodology for the estimation of terrestrial net primary prodcution from remotely sensed data, *J. Geogr. Res., 99*, 5263-5283, 1994.

Ruimy, A., G. Dedieu, and B. Saugier, TURC: A diagnostic model of continental gross primary productivity and net primary productivity, *Global Biogeochem. Cycle, 10*, 269-285, 1996.

Running, S. W., and J. C. Coughlan, A general model of forest ecosystem processes for regional applications, I, Hydrological balance, canopy gas exchange and primary production processes, *Ecol. Modell., 42*, 125-154, 1988.

Running, S. W., and E. R. Hunt, Generalization of a forest ecosystem process model for other biomes, BIOME-BGC, and an application for global scale models, in *Scaling Physiological Processes: Leaf to Globe*, edited by J. R. Ehleringer and C. B. Field, pp. 141-158, Academic, San Diego, Calif., 1993.

Running, S. W., R. R. Nemani, D. L. Peterson, L. E. Band, D. F. Potts, L. L. Pierce, and M. A. Spanner, Mapping regional forest evapotranspiration and photosynthesis by coupling satellite data with ecosystem simulation, *Ecology, 70*, 1090-1101, 1989.

Ryan, M. G., Growth and maintenance respiration in stems of *Pinus contorta and Picea engelmannii*, *Can. J. For. Res., 20*, 48-57, 1990.

Ryan, M. G., A simple method for estimating gross carbon budgets for vegetation in forest ecosystems, *Tree Physiol., 9*, 255-266, 1991.

Ryan, M., M. B. Lavigne, and S. T. Gower, Annual carbon cost of autotrophic respiration in boreal forest ecosystems in relation to species and climate, *J. Geophys. Res., 102*, 28,871-28,883, 1997.

Sellers, P. J., J. A. Berry, G. J. Collatz, C. B. Field, and F. G. Hall, Canopy reflectance, photosynthesis, and transpiration, III, A reanalysis using improved leaf models and a new canopy integration scheme, *Remote Sens. Environ., 42*, 187-216, 1992.

Sellers, et al., The Boreal Ecosystem-Atmosphere Study (BOREAS): An overview and early results from the 1994 field year, *Bull. Ame. Meteorol. Soc., 76*, 1549-1548, 1995.

Sellers, P. J., D. A. Randall, G. J. Collatz, J. A. Berry, C. B. Field, D. A. Dazlich, C. Zhang, G. D. Collelo, and L. Bounoua, A revised land surface parameterization (SiB2) for atmospheric GCMs, I, Model formulation, *J. Clim., 9*, 676-705, 1996.

Sellers, P., et al., BOREAS in 1997: Scientific results, overview, and future directions, *J. Geophys. Res., 102*, 28,731-28,769, 1997.

Shields, J. A., C. Tarnocai, K. W. G. Valentine, and K. B. MacDonald, Soil landscapes of Canada, procedures manual and user's hand book, Agric. Can. Publ. 1868/E, Agric. Can., Ottawa, Ontario. 1991.

Snyder, J. P., Map projections--a working manual, U.S. Geol. Surv. Prof. Pap., *I 19.16:1395*, U.S. Gov. Prin. Off., Washington, D. C., 1989.

Steele, S. J., S. T. Gower, J. G. Vogel, and J. M. Norman, Root mass, net primary production and turnover in aspen, jack pine and black spruce forests in Saskatchewan and Manitoba, Canada, *Tree Physiol., 17*, 577-587,1997.

Wiegand, C. L., S. J. Maas, J. K. Aase, J. L. Hatfield, P. J. Pinter Jr., R. D. Jackson, E. T. Kanemasu, and R. L. Lapitan, Multisite analyses of spectral-biophysical data for wheat, *Remote Sens. Environ., 42*, 1-21, 1992.

Woodward, F. I., T. M. Smith, and W. R. Emanuel, A global land primary productivity and phytogeography model, *Global Biogeochem. Cycle, 9*, 471-490, 1995.

Wullschleger, S. D., Biochemical limitations to carbon assimilation in C_3 plants - A retrospective analysis of the A/C_i curves from 109 species, *J. Exp. Bot., 44*, 907-920, 1993.

J. M. Chen, W. Chen, J.Cihlar, and J. Liu, Canada Centre for Remote Sensing, 588 Booth Street, Ottawa, Ontario, Canada, K1A 0Y7. (e-mail: jliu@ccrs.nrcan.gc.ca).

(Received April 13, 1999; revised July 15, 1999;
accepted July 19, 1999.)